PREPRINT UCRL- 83488

CONF-791112--25

Lawrence Livermore Laboratory

COMPUTER MODELING OF NUCLEAR WASTE STORAGE CANISTER CORROSION

Peter T. Cottrell, Wesley D. Ludemann and R. Daniel McCright

October 18, 1979

Prepared for the Scientific Basis for Waste Management, Boston, Massachusetts, November 22-26, 1979.

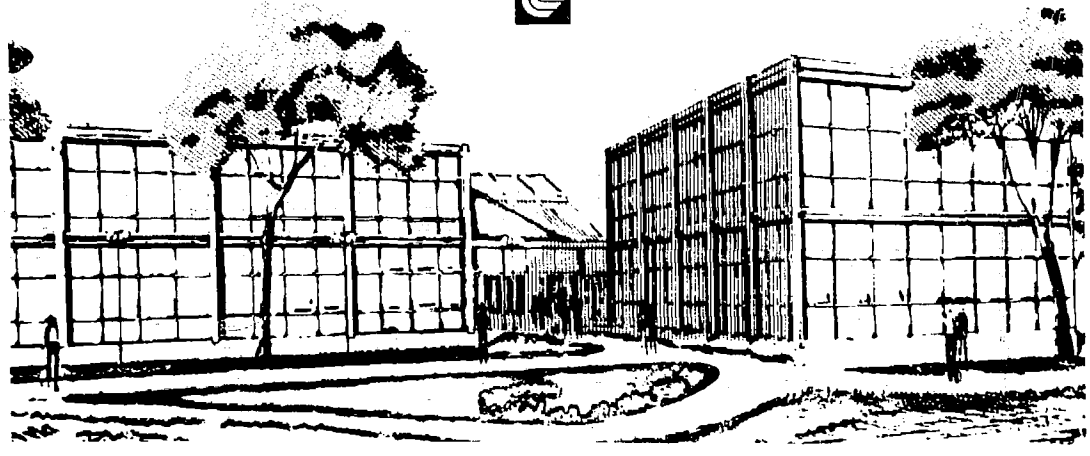

COMPUTER MODELING OF NUCLEAR WASTE STORAGE CANISTER CORROSION †

Peter T. Cottrell*, Wesley D. Ludemann and R. Daniel McCright

ABSTRACT

Current plans for nuclear waste disposal include placing the waste in a canister to isolate it from the repository environment for 1000 years. Corrosion prediction techniques are currently inadequate to guarantee the canister performance over this length of time. We are attempting to better predict the corrosion process with the help of computer modeling. We developed a program to calculate anodic and cathodic polarization curves using Tafel slopes, equilibrium exchange current densities, and other electrochemical parameters obtained from the experimental corrosion literature. The model generates and displays polarization curves for different values of environmental parameters such as temperature, pH, and concentrations of pertinent species in the vicinity of the canister material. For the case of uniform corrosion in acidic media, our model predicts corrosion rates in fair agreement with literature values. Our modeling effort is at present only applicable to the uniform corrosion situation. Fundamental theoretical and experimental research is necessary before models can be developed to handle passivating layers or non-uniform corrosion.

Radioactive waste must be isolated from the biosphere until radioactive decay reduces the residual radioactivity to a very low level. The disposal option currently favored is burial in a geological medium. Several barriers to radionuclide migration can be provided with this option. The nuclear waste is first vitrified or converted to another form which has very low solubility in ground waters. This solidified waste is then placed in a protective canister, and the canister is stored in a repository in a geological formation which has, among other characteristics, a low permeability. Radioactive material then can enter the biosphere only after a sequence of events which includes corrosion of the canister, dissolution of the waste, and migration of the dissolved waste to the biosphere. This sequence must take sufficiently long for the released waste to attain an acceptably low level of radioactivity.

* Currently at Department of Chemistry, Florida A & M University, Tallahassee, Florida 32307

† This work was supported by the U.S. Nuclear Regulatory Commission under Interagency Agreement DOE 40-550-75 with the U.S. Department of Energy.

Short-lived products of fission and activation are relatively mobile whereas the longer-lived actinides migrate much more slowly. The role of the canister is to isolate waste from the repository environment until these short-lived isotopes decay. Perhaps 1000 years isolation will be required for decay of the ^{137}Cs and ^{90}Sr isotopes. Since the canister provides the 1000 year isolation, knowledge of its performance is essential.

It is easy to state a corrosion performance criterion for a waste storage canister; it is simply, no breach for 1000 years. It is more difficult to specify acceptance criteria, however, as our current knowledge is insufficient to assure integrity over this length of time. Twenty years is found to be a long time over which to predict corrosion performance on the basis of short term and accelerated corrosion tests. To extend our predictive ability by one to two orders of magnitude is a large task. Research needs include the development of very sensitive corrosion monitoring techniques and accelerated corrosion testing methods. The effects of radiolysis on corrosion, especially in the presence of chlorides, must be determined, and longterm corrosion mechanisms must be identified.

Even with new experimental techniques, the prediction of corrosion behavior over a millenium will be a difficult task. For this reason it is necessary to develop an ability to extend the range and degree of confidence of corrosion prediction. Toward this end we started work on a calculational model for predicting changes in corrosion rate with changing environmental conditions.

In the complete model we will use the canister composition, the repository ground water composition, and the thermal and radiation fluxes from the waste as input parameters. The first step is to calculate changes in the chemical environment due to heat and radiolysis. The next step is to calculate the polarization curves, and from these obtain the instantaneous rate of corrosion. Since the corrosion rate depends on the environment, we must then make calculations which take into account the changing conditions along with the buildup of protective films on the canister. After making these changes, the new corrosion rate is calculated, and the process repeated as many times as necessary. Summation of the metal wastage after each loop of the calculation gives the total metal penetration. While our work so far has been limited to the simple case of iron corroding in acid solutions, we have established the method of generating polarization curves as a function of the input variables.

When a metal such as iron is placed in a electrolyte, the following reaction occurs:

$$Fe \rightleftharpoons Fe^{++} + 2e$$

The forward reaction leads to corrosion and the reverse reaction to plating. At the equilibrium potential the two reactions are of equal magnitude and there is no net current flow. If the electrode potential is displaced from its equilibrium value, current flows preferentially in one direction and the metal is either oxidized or plated. The familiar polarization diagram is obtained by plotting the electrode potential against the logarithm of the current density. The slope of the linear portion of the curve is called the Tafel slope, and the displacement of the potential from equilibrium is the overpotential.

During corrosion, the iron potential is shifted so that the oxidation reaction predominates. The concurrent reduction reaction is usually either the hydrogen evolution reaction or the oxygen reduction reaction. Since anode and cathode are in electrical contact, the potentials for all reactions shift from their equilibrium values to a common value, the corrosion potential. At this potential the net current flowing in the circuit is the corrosion current. The number of equivalents of iron dissolved are equal to the number of equivalents of hydrogen liberated, and, by Faraday's law, the corrosion penetration rate can be calculated in mm/yr.

The Tafel slope of a reaction is a measure of the difficulty of transferring an electron at the interface during the reaction. The more difficult the transfer step is, the steeper is the slope and the lower is the corrosion current. The overpotential resulting from electron transfer is called the activation overpotential, since an activation barrier must be surmounted. Other factors may also limit the corrosion rate. Slowness of mass transport gives rise to a transport overpotential, and the electrical resistance of the cell which gives rise to a resistance overpotential.

In our calculations we refer all potentials to the standard hydrogen electrode as a reference. Thus the equilibrium potential at 298°K is -0.44 volts for Fe/Fe^{++} and is +1.22 volts for H_2O/O_2.

We calculate the activation potential η_A in the following manner. Since the net current density i is the difference between the anode and cathodic current densities for a given reaction,

$$i = i_{anodic} - i_{cathode}.$$

From the basic electrode or Butler-Volmer equation,

$$i = i_o \left[\exp \frac{(1-\beta)\, n_A\, zF}{RT} - \exp \frac{-\beta\, n_A zF}{RT} \right]$$

where i_o = equilibrium exchange current density

β = symmetry factor (~ 0.5)

z = number of electrons transferred

F = Faraday constant (96,487 coulombs/mole)

R = Gas constant (8.31 Joules/mole ^oK)

T = Absolute temperature

For metal dissolution at apppreciable rates,

$$i_{anodic} >> i_{cathodic}$$

So that

$$i = i_o \exp \frac{(1-\beta) n_A\, zF}{RT}$$

and the activation overpotential is

$$n_A = - \frac{RT}{(1-\beta)\, zF} \log i_o + \frac{RT}{(1-\beta) zF} \log i$$

Note that $n_A = 0$ at $i = i_o$,

and that the Tafel slope is $\frac{RT}{(1-\beta)\, zF}$

For $\beta = 0.5$, the Tafel slope is $\frac{0.59}{z}$

The equilibrium potential depends on the temperature and concentration of the ferrous ion,

$$E_o = -0.49 + \frac{0.59}{z} \frac{T}{298} \log [Fe^{++}]$$

The exchange current density and the equilibrium potential give the starting point for the polarization diagram.

The exchange current density i_o depends on the size and shape of the activation barrier, the temperature and the concentrations of the species undergoing the electron transfer, so that

$$i_o = \text{constant} \cdot T\, C_{ox}^{(1-\beta)}\, C_{red}^{\beta} \exp(-\Delta H^{\ddagger}/RT)$$

where C_{ox} = concentration of the oxidized species ,

C_{red} = concentration of the reduced species

$\Delta H^{\ddagger}$ = enthalpy at activation

Experimentally, Hurlen[1] has found for Fe/Fe^{++} that

$$\log i_{o,\,298} = 3.58 - pOH - pFe$$

and for H^+/H_2

$$\log i_{o,\,298} = 5.36 - 0.5pH$$

so that at a temperature T

$$\log i_o = \log i_{o,\,298} + \log \frac{T}{298} + \frac{\Delta H^{\ddagger}}{R} \cdot \frac{T-298}{298T}$$

The transport overpotential η_T depends on the limiting current i_L:

$$\eta_T = \frac{RT}{zF} \ln \left(1 - \frac{i}{i_L}\right)$$

For hydrogen evolution,

$$i_L = 0.144 \frac{T}{298}$$

The resistance overpotential η_R is proportional to the cell resistance,

$$\eta_R = iR$$

and is negligible except for high resistance and high current densities.

The total overpotential η is thus

$$\eta = \eta_A + \eta_T + \eta_R$$

We tested the computer program by calculating a number of polarization diagrams using arbitrarily selected parameters. The type of result we obtained is illustrated in figure 1, which shows polarization curves for Fe/Fe^{++} (positive slope), H_2/O_2 (negative slope, upper curve) and H^+/H_2 (negative slope, lower curve). The sum of the two cathodic reactions is given by the curve marked with X's. The contribution of the H^+/H_2 reaction to the sum is negligible at low current densities and becomes important only at higher current densities. The intersection of the anodic curve with the sum of the cathodic curves gives the corrosion current density and the corrosion potential. Activation overpotential controls over the linear segment of each curve. Transport overpotential limits the total amount current that can flow, and results in the vertical segment of each curve. Resistance overpotential causes a slight rounding of the polarization curves, and is noticeable only at high current densities.

In figures 2 through 5 we varied different parameters individually to show the effect of their variation. In each case we show only the sum of the two cathodic reactions along with the anodic reaction.

The effect of pH variation in an anoxic solution is shown in figure 2. The lower the pH, the higher the corrosion current. At high current densities, the effect of resistance polarization can be seen in the hydrogen polarization curves.

The effect of oxygen concentration variation is shown in figure 3 for a rather low hydrogen ion content. As the oxygen concentration decreases, hydrogen evolution replaces oxygen reduction as the dominant cathodic reaction.

The effect of metal ion concentration variation is shown in figure 4. At lower metal ion concentrations the reaction is activation controlled, while at higher concentrations, it is transport controlled.

The effect of temperature variation is shown in figure 5. It affects the Tafel slope and the limiting densities of both the anodic and cathodic reactions.

The effect of cell resistance is shown in figure 6. The higher the resistance, the lower the corrosion current.

In conclusion, we believe that where the mechanisms of corrosion are known, a calculational model such as the above will be of value in improving our ability to predict corrosion rates. An extension of this model to take into account temporal changes in environment and on the corroding surface will aid in making long term predictions.

Reference

1. "Electrochemical Behavior of Iron", Tor Hurlen, Act. Chem Scand. 14, (1960) 1533-54.

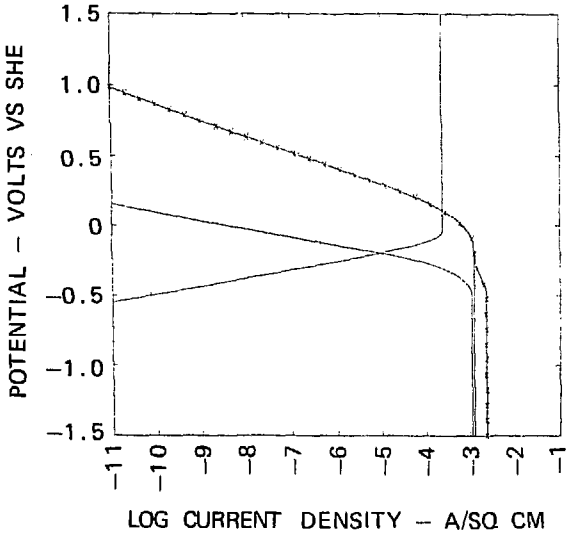

FIG. 1. A calculated polarization diagram for iron corroding in an oxygen saturated acidic solution.

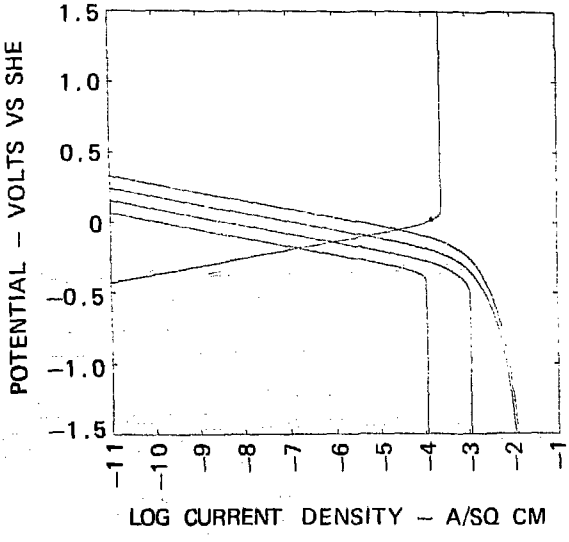

FIG. 2 The effect of pH variation on the corrosion of iron in an anoxic solution.

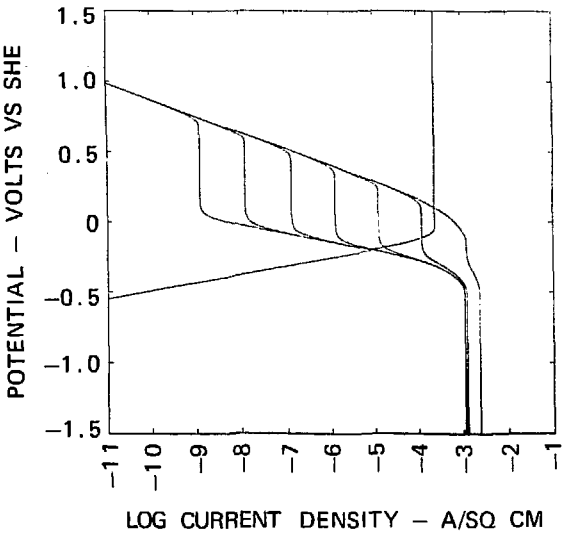

FIG. 3. The effect of oxygen variation on the corrosion of iron in an acidic solution.

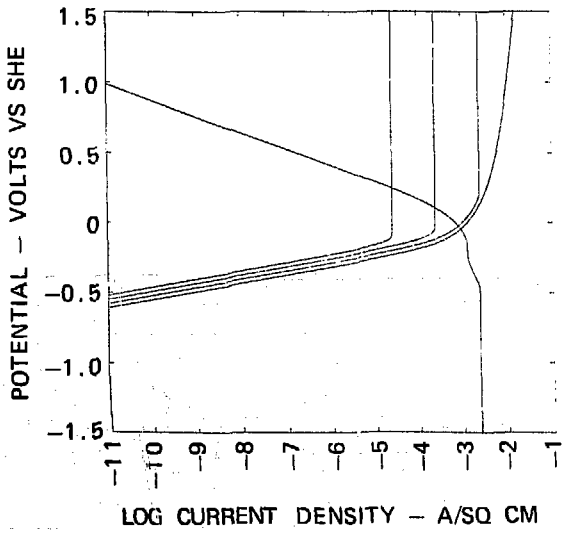

FIG. 4. The effect of Fe^{++} concentration on the corrosion of iron in an oxygen saturated acidic solution.

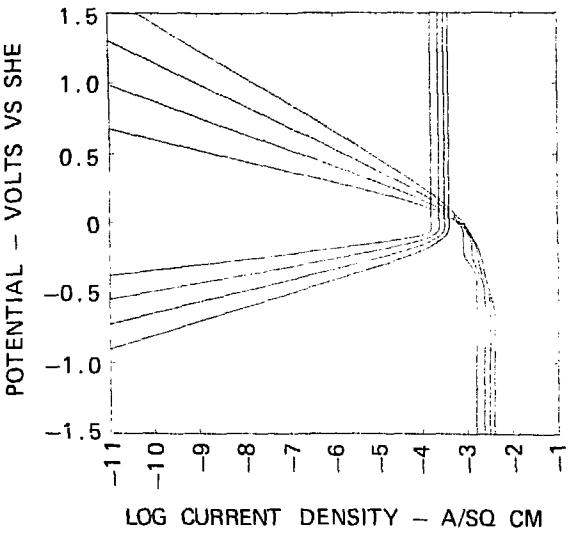

FIG. 5. The effect of temperature on the corrosion of iron in an oxygen saturated acidic solution.

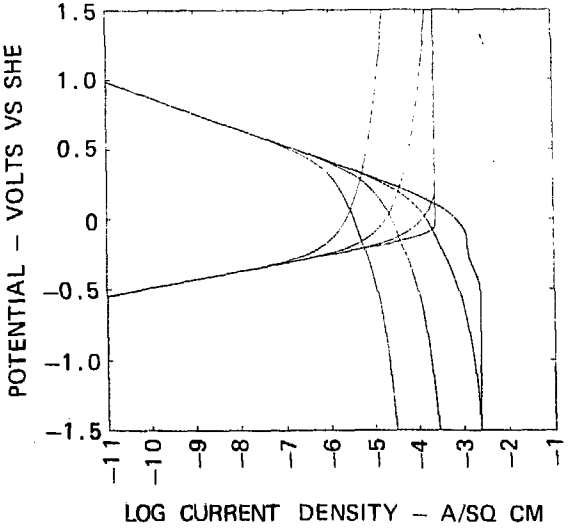

FIG. 6 The effect of cell resistance on the corrosion of iron in an oxygen saturated acidic solution.